

# ANALYSIS OF INFRARED LIGHT TRAPPING ON BIFACIAL SILICON HETEROJUNCTION SOLAR CELLS

Félix Gérenton\*, Samuel Harrison, Perrine Carroy, Anthony Valla, Adrien Danel, Delfina Muñoz  
Univ Grenoble Alpes, CEA, LITEN, INES, F-38000 Grenoble

\*Corresponding author: [felix.gerenton@cea.fr](mailto:felix.gerenton@cea.fr); Phone: +33.479.79.28.42

**ABSTRACT:** In silicon heterojunction (SHJ) solar cells, the transparent conductive oxide (TCO) layers used are designed to balance resistive losses and parasitic light absorption. This paper aims to determine the rear TCO optimization that can be made in the case of bifacial SHJ cells, taking into account both optical and electrical aspects. First, internal reflectance in bifacial cells is simulated and characterized for more or less transparent TCO layers, and compared to monofacial cells, in order to establish if the use of a more transparent TCO layer stays beneficial for bifacial cells as well. Then, the internal reflectance is further optimized by tuning the TCO thickness. In this work, we thus show that using a more transparent ITO layer remains an important path of improvement for the internal reflectance in bifacial cells, and that TCO thickness should be optimized differently than for monofacial cells. These results have been confirmed at cell level with a gain in short-circuit current without significant resistive losses observed, resulting in a final efficiency gain. Moreover, this optimization is proved to be also beneficial for the cell's bifaciality behavior.

**Keywords:** bifacial cells; heterojunction; transparent conductive oxide; light trapping; indium-tin oxide

## 1 INTRODUCTION

Silicon heterojunction (SHJ) solar cells have the advantages of both great conversion efficiencies [1] and high in-field performances, especially in the case of bifacial cells, where the sunlight reverberated behind a solar panel can be converted into electrical power as well. Moreover, the bifacial configuration does not require any additional step for SHJ cells fabrication [2], and uses much less metal paste.

In a bifacial SHJ cell, a metal grid is printed on both front and rear sides (Fig. 1a), and the pitch between two fingers should be optimized to limit both optical losses through shadowing, and resistive losses through lateral conduction. However, the impact of these two factors on conversion efficiency is quite different whether we consider front or rear cell side, as the amount of light received on the rear is much lower than the front (10 to 20% of the sunlight on typical field installations). In order to maximize the power output, it is thus preferable to use a smaller pitch on the rear side, resulting in a smaller photogenerated current at the rear but less resistive losses, which is more critical as it impacts also the cell power generated from the front side. Typical cell performances and associated bifaciality coefficient (ratio of efficiencies from the rear / from the front) with different rear grid pitches are shown in Fig. 1b.

The transparent conductive oxide layer (TCO), used for optical confinement and for carrier transport between the amorphous silicon (a-Si:H) contacts and the metal grid, needs to be optimized to balance its lateral conductivity and parasitic absorption in near-infrared (NIR) [3]. In the general case of a cell with a denser metal grid at the rear, front and rear TCO layers could be optimized differently. Indeed, the lateral conductivity of the rear TCO becomes less critical for the device, and a layer with a lower NIR absorption could reduce the optical losses, as described in [4] for monofacial cells, without critically increasing the resistive losses.

This study will first focus on the behavior of infrared light into a bifacial SHJ cell and will highlight the differences with monofacial cells, through optical simulations and characterizations, in order to understand the possible optimization paths for a rear TCO layer in a bifacial cell. Then, TCOs with different optical and

electrical properties will be integrated into bifacial SHJ cells in order to evaluate its impact on different cells parameters, especially short-circuit current ( $J_{sc}$ ), fill factor (FF), conversion efficiency and bifaciality coefficient.

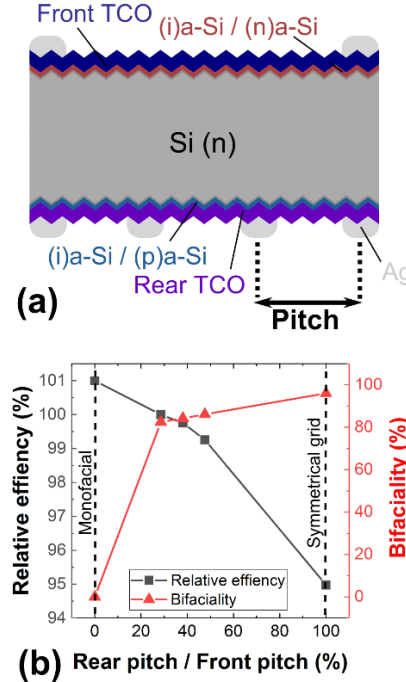


**Figure 1:** (a) Representation of a bifacial SHJ cell. (b) Typical SHJ cell relative efficiency and bifaciality for different rear grid pitches.

## 2 MATERIAL AND SOLAR CELL PROCESSES

### 2.1 Fabrication of low-absorption TCO layers

This work focuses on the optimization of indium-tin oxide (ITO) layers, which is the most usual among the possible TCO materials used in SHJ cell process [5]. These layers are deposited by magnetron sputtering from an  $\text{In}_2\text{O}_3/\text{SnO}_2$  target, under an  $\text{Ar}/\text{O}_2$  gas mixture. The material properties are modified by changing the  $\text{O}_2$  flow in the deposition chamber, from 8 to 24 sccm. The Ar flow stays fixed at 500 sccm. As the deposition rate is sensitive to the gas ratio in the chamber, the deposition time is

adjusted to keep a fixed targeted thickness for all conditions (100 nm on polished substrate, unless stated otherwise). In order to reproduce the thermal step of metal paste curing in the cell process, all the layers are annealed at 205 °C for 9 min. Depositions are made simultaneously on polished silicon, glass and SHJ solar cells.

The different layers are characterized by spectroscopic ellipsometry using a combination of Tauc-Lorentz and Drude models [6], reflectometry (on glass samples), and Hall effect measurements. The absorbance vs wavelength, the carrier concentration ( $N$ ) and the resistivity of the different ITO layers are summarized in Fig. 2.

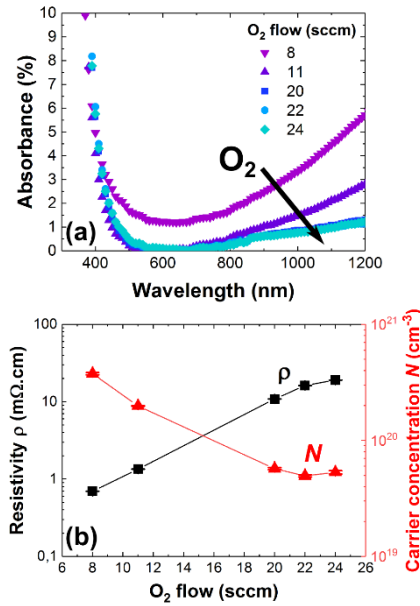


**Figure 2:** (a) Absorbance in ITO layer vs. wavelength for different O<sub>2</sub> flows. (b) ITO resistivity  $\rho$  and carrier concentration  $N$ .

As usually observed [3-4], the absorbance in NIR range decreases as the O<sub>2</sub> flow increases. In this case, absorbance does not evolve from 20 to 24 sccm of O<sub>2</sub>. The ITO resistivity still increases with O<sub>2</sub> until 24 sccm, even though carrier concentration stays quite constant from 20 to 24 sccm. The explanation stands in the mobility that keeps decreasing up to 24 sccm (not shown).

Therefore, the TCO layers deposited with an O<sub>2</sub> flow higher than 20 sccm are of no interest for integration in SHJ cells, as parasitic NIR absorption does not decrease anymore, and series resistance could increase because of the increased ITO resistivity. For the sake of simplicity, the following studies will focus on ITO layers deposited with an O<sub>2</sub> flow of 8 and 20 sccm, which will be called “high- $N$ ” and “low- $N$ ” respectively, representing their respective carrier concentrations  $N$ , of very different values.

## 2.2 Solar cell process

All the cells realized in this study are based on n-type wafers with a resistivity of 2.5 Ω.cm. Substrates are cleaned and textured, with a final thickness of 165 μm. Doped and intrinsic amorphous silicon (a-Si:H) layers are deposited on both sides, with n-type doping on the front side and p-type on the rear (“inverted emitter” architecture [3]). ITO is then deposited on the front and the rear side, with different sets of parameters for the rear as described

in 2.1. Metal grids are screen-printed from a silver paste, with a 4 busbars pattern, a finger pitch of 2.1 mm on the front and 0.6 mm on the rear. After screen-printing, all cells are annealed at 205 °C for 9 min in order to cure the silver paste. Finally, all cells are characterized in current-voltage (IV) with probe bars on both sides, without a metal chuck in order to avoid parasitic reflections at the back of the cell. IV characterizations are made on both sides of the cell in order to extract bifaciality coefficients. More details about the cell process can be found in [2].

## 3 LIGHT PROPAGATION IN BIFACIAL SHJ CELLS

This part aims to give insights on the main differences in light interaction with the cell’s rear side in the case of monofacial and bifacial cells. This analysis allows then to highlight the preferential optimization paths for the rear TCO layer in order to reduce the optical losses in a bifacial cell.

### 3.1 Internal reflectance: effect of material properties

In order to understand how the light propagates at the rear of mono- and bifacial cells for different TCO properties (high- $N$  and low- $N$  in this study), simulations of internal reflectance, absorbance and transmittance (R/A/T) are performed with a variable incident angle, on the online simulator OPAL 2 [7]. This calculator is based on the solving of the Fresnel equations [8] to compute R/A/T in a layer or stack of layers between two semi-infinite media. Here, we consider a layer of ITO with a complex refractive index measured with ellipsometry, and a thickness of 73.5 nm (thickness measured of 98.2 nm on flat substrate, converted to the thickness on textured substrate). a-Si:H layers are omitted, as they are transparent in the infrared range. The ambient media is silicon, and the external media is silver or air for mono- and bifacial cells respectively. Simulations are realized at a wavelength of 1200 nm and an angle varying from 0 to 90°.

Differentiation of light propagation regimes in the Si-ITO-air system occurs at two critical angles. First, the escape angle  $\theta_e = \sin^{-1}(1/n_{Si})$  where  $n_{Si}$  is the refractive index of silicon, above which light is totally reflected at the ITO/air interface. Then, the total reflection angle  $\theta_r = \sin^{-1}(n_{ITO}/n_{Si})$  with  $n_{ITO}$  being the refractive index of the ITO layer considered, above which light is totally reflected at the Si/ITO interface. One should note that even above  $\theta_r$ , absorption in ITO is expected as light is still going through the ITO layer on the form of an evanescent wave [4]. For the Si-ITO-silver system corresponding to the monofacial case, the only angle separating different propagation regimes is  $\theta_r$ . All cases are summarized in Fig. 3.

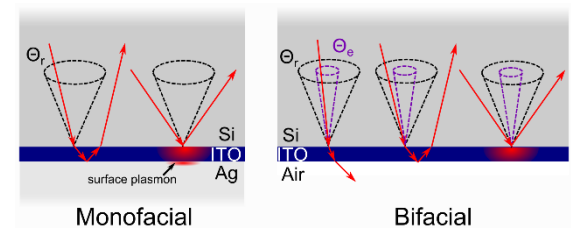


**Figure 3:** Representation of the different light propagation modes at the rear interface of mono- and bifacial SHJ cells.

R/A/T simulations results are presented in Fig. 4. The monofacial case presents, as already described in the

literature [4], a peak of absorbance occurring at intermediate angles, above  $\theta_r$ . This effect is known to come from the penetration of *p*-polarized waves interacting with the metal [9]. In our case, reflection is improved for all angles with low-*N* ITO. This is not a systematic rule, as the absorption peak shifts with the refractive index, the reflectance could be higher with a less transparent ITO on high angles. Moreover, in our case, absorption in silver is low compared to the ITO, which is not always the case.

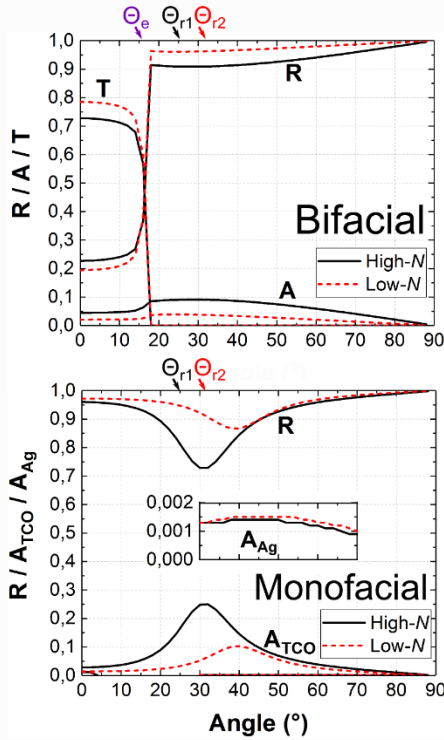


**Figure 4:** Reflectance, absorbance in ITO and transmittance (bifacial) or absorbance in silver (monofacial) versus incident angle for Si-ITO-air and Si/ITO/Ag systems.  $\theta_{r1}$  and  $\theta_{r2}$  are the total refraction angles for high-*N* and low-*N* ITO respectively.

The bifacial case behaves differently: from normal incidence to  $\theta_e$ , where most of the light is transmitted into the air, reflectance is higher for the high-*N* ITO. This comes from a reduced transmittance to air, itself due to a lower refractive index value, increasing reflectance both at the Si/ITO and ITO/air interface. After  $\theta_e$ , no light is transmitted outside of the cell, and parasitic absorption exists whether waves can propagate to the ITO (below  $\theta_r$ ) or are totally reflected (above  $\theta_r$ ), with an evanescent field decaying through the ITO layer. However, absorbance is lower for low-*N* ITO, which means that the value of  $\theta_r$ , driven by  $n_{ITO}$ , has little influence on internal reflectance compared to the ITO absorption, driven by the extinction coefficient  $k_{ITO}$ . Moreover, the interaction with the air interface is very different from a metal, which is observed by the absence of the absorption peak present on the monofacial case.

Consequently, the ideal ITO layer for the rear side of a bifacial cell is ambiguous: depending on the incident angle with respect to  $\theta_e$ , the reflectance can be improved with either a high-*N* or a low-*N* material. Therefore, the choice of material depends on the angular distribution of rays arriving at the rear interface. In order to determine the

best material in this case, reflectometry is performed on cells, monofacial and bifacial, with high-*N* and low-*N* ITO on the rear (Fig. 5).

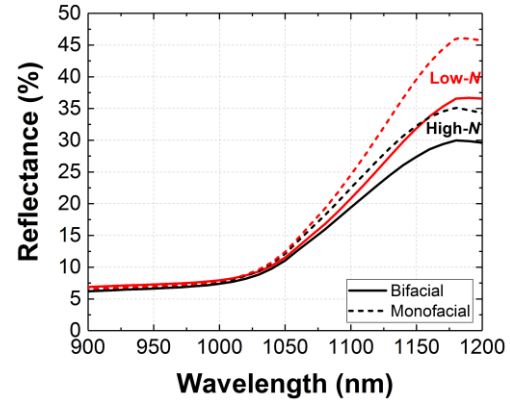


**Figure 5:** SHJ cell reflectance versus wavelength, for bifacial and monofacial cases, with high-*N* and low-*N* ITO on the rear side.

An important gain in reflectance at the cell level is observed by using a low-*N* ITO, for both monofacial and bifacial cells, even if the gain is higher for monofacial cells. This implies that in the case of a SHJ cell textured on both sides, the angles taken by the rays on the rear side are globally large enough to make the gain in internal reflectance for low-*N* ITO larger than the losses. This observation is verified at every wavelength in the 1000-1200 nm range, confirming a global reflectance improvement in the infrared. A consequence of this observation is that even if light can escape from the cell by the rear side, optimizing the TCO properties on the rear of bifacial cells still allows a large gain in reflectance.

Moreover, these reflectance gains translate well to external quantum efficiency (EQE) measurements in the infrared (Fig. 6), confirming a gain in  $J_{sc}$  by using a low-*N* ITO on bifacial cells.

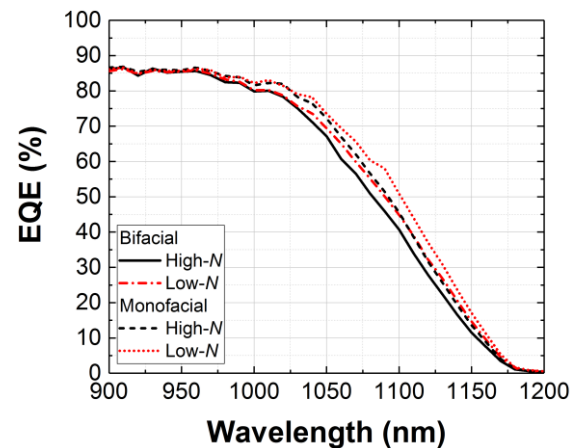


**Figure 6:** EQE in the infrared range for bifacial and monofacial cells with high-*N* and low-*N* ITO layers at the rear

### 3.2 Internal reflectance: effect of rear TCO thickness

On monofacial cells, optimizing the thickness of the rear TCO layer can be critical: evanescent waves can be absorbed through surface plasmons in the metal layer underneath if the ITO is too thin, or in the ITO itself with an excessive thickness [4]. In bifacial cells, no plasmon

losses occur, and reflectance varies with angle in a very different way than monofacial cells, as already shown in Fig. 4. Therefore, the R/A/T values for different ITO thicknesses should be reassessed in the case of bifacial cells. For this purpose, we perform R/A/T simulations of a Si/ITO/air system on OPAL 2, focusing on a low- $N$  ITO layer with three different thicknesses: 73.5, 147 and 220.5 nm (corresponding to the reference thickness of 73.5 nm used in 3.1, and this value multiplied by 2 and 3). Equivalent simulations for a monofacial case are performed as well. Results are shown in Fig. 7.

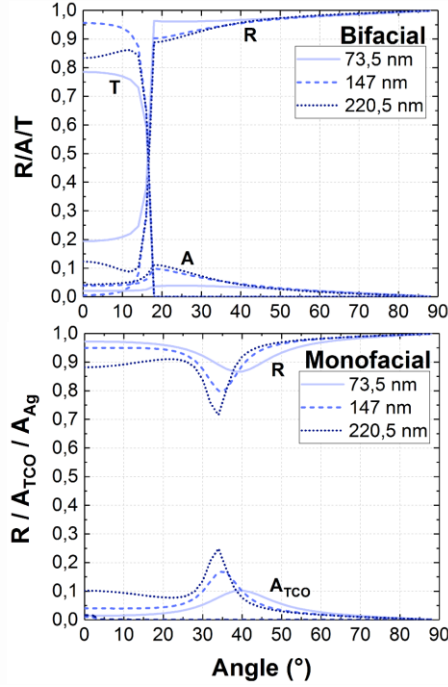


**Figure 7:** R/A/T versus incident angle for Si-ITO-air and Si/ITO/Ag systems.

As for the study on materials properties (see 3.1), monofacial and bifacial reflectors behave very differently with different ITO thicknesses. For the monofacial case, the absorbance peak shifts to lower angles with increasing ITO thickness, making the best thickness for internal reflectance very dependent on the angular distribution. For the bifacial case, the reflectance is clearly improved at all angles for a thinner layer, decreasing both absorbance due to a smaller pathlength in the ITO, and transmittance at low incidence angles due to interference effects. Here again, these angle-dependent behaviors are now assessed on finished devices in order to analyze the TCO thickness impact on internal reflectance for a textured cell (Fig. 8).

For the monofacial case, the reflectance measurements confirm the high dependence of the response with the angle distribution: on a textured cell, the difference of global reflectance between different ITO thicknesses is quite small, and is not measurable on EQE.

For the bifacial case, the R/A/T graphs (Fig. 7) translate also well to global reflectance and EQE: with the thinner ITO layer, both reflectance and EQE are improved in the infrared, while the two higher thicknesses give very close responses.

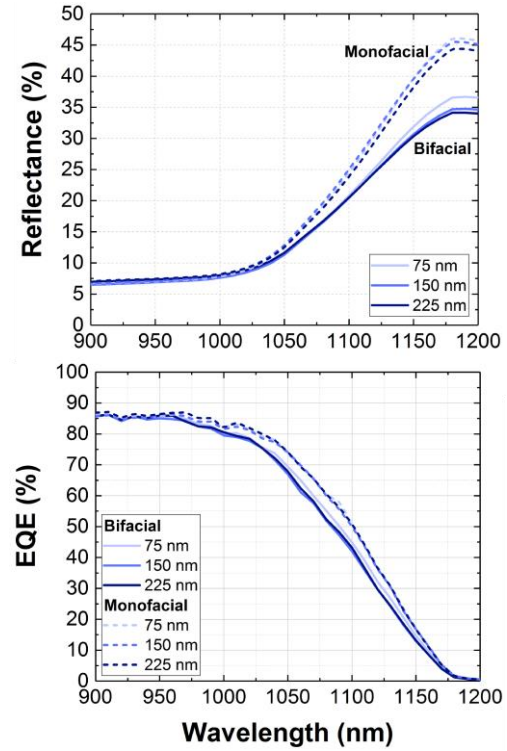


**Figure 8:** SHJ cell reflectance (top) and EQE (bottom) versus wavelength, for bifacial and monofacial cases, with ITO thicknesses of 75, 150 and 225 nm.

Finally, one can conclude that bifacial cells tend to have an improved internal reflectance with a thinner layer because of the very different light propagation mechanisms at the rear compared to monofacial cells. More precisely, reflectance above the escape angle  $\theta_e$  is improved with a thinner layer because of the reduced pathlength into the TCO layer, while in monofacial cells, the absorbance peak shifts with thickness, making the response with angle more ambiguous. Therefore, even if some interference effects exist on bifacial cells, especially at angles below  $\theta_e$  (Fig. 7), internal reflectance in bifacial cells is improved by a thinner layer on a wider angle range than monofacial cells, and consequently, on a textured device, internal reflectance rises with a thinner TCO layer. In our work, as the reference thickness used ( $\sim 75$  nm on textured substrate) demonstrated better results than the thicker layers, it will be chosen for the rest of the study.

#### 4 PERFORMANCES OF BIFACIAL CELLS WITH OPTIMIZED REAR TCO

Two batches of 17 cells are fabricated with high- $N$  and low- $N$  layers. IV results and bifaciality coefficients are presented in Fig. 9.

$V_{oc}$  does not evolve significantly between both sets of cells (1 mV of difference).  $J_{sc}$  increases by 0.2 mA/cm<sup>2</sup> for low- $N$  ITO, confirming the gain in internal reflectance and quantum efficiency observed in 3.1. The fill factor (FF) drops in average by 0.2%<sub>abs</sub>, but with a quite large variability within each batch, as the standard deviation is 0.8 and 1.2%<sub>abs</sub> for high- $N$  and low- $N$  ITO respectively. Finally, the efficiency rises by 0.1%<sub>abs</sub> by using a low- $N$  ITO. It is worth noting that this result is potentially very dependent on the rear finger pitch, fixed at 0.6 mm here.

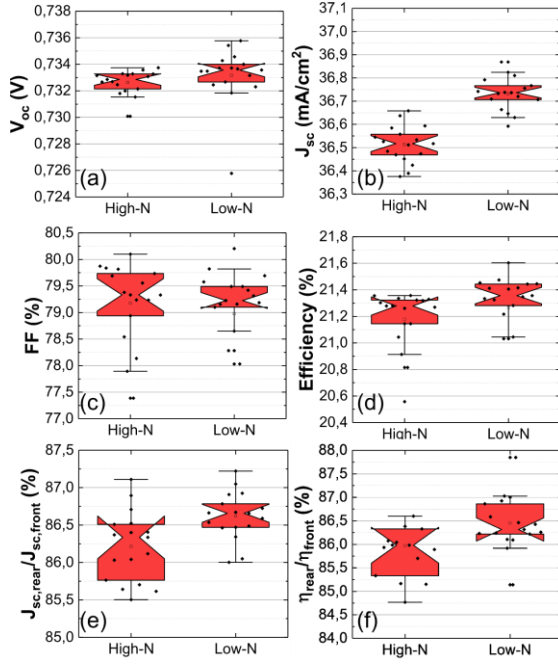


**Figure 9:** IV characteristics (a-d) and bifaciality coefficients (e-f) for SHJ cells with high-*N* and low-*N* ITO on the rear.

A second batch of cells realized in very similar conditions, with only slightly different ITO thicknesses (97 and 90 nm for high-*N* and low-*N* respectively) showed similar performances, in particular 0.3 mA/cm<sup>2</sup> in  $J_{sc}$ , +0.0%<sub>abs</sub> in FF and +0.1%<sub>abs</sub> in efficiency.

Finally, bifaciality slightly improves as well with a low-*N* ITO (Fig. 9f), going from 86.0% to 86.5% in average. This is due to the lower NIR parasitic absorption, which also improves current photogeneration when the cell is illuminated from the rear, as demonstrated in [4] for front-side TCO layers. This is confirmed by the improved bifaciality coefficient of  $J_{sc}$  (Fig. 9e), matching very well the improved global bifaciality.

## 5 CONCLUSION

The objective of this work was to assess if the possible optimizations of the rear TCO on monofacial SHJ cells stay valid for bifacial cells to some extent. In the practical case of bifacial cells with a smaller grid pitch on the rear side, the lateral conduction properties of the ITO are less critical, giving the possibility to improve  $J_{sc}$  by using a more resistive and more transparent layer.

The first objective was to verify how light propagates at the rear of a bifacial cell, and if a more transparent layer would improve internal reflectance. Through internal reflectance/absorbance/transmittance simulations, we showed that the propagation of light is very different on bifacial and monofacial cells. Especially, transmittance outside the cell is important at low incidence angles, and reflectance/absorbance are found quite different than monofacial cells for other angles. Moreover, in both cases, the internal reflectance of a device is dependent on the angle distribution at the rear. However, on a textured SHJ cell, we showed that internal reflectance is improved in the whole infrared range for a more transparent TCO. Consequently, even with the possibility of light escape at the rear of a bifacial cell, the internal reflectance can be improved in the same way than for a monofacial cell.

Another aspect to optimize was the TCO thickness. After similar investigations on internal reflectance, it appeared that monofacial or bifacial configurations respond very differently with respect to the incident light angle. At cell level, the reflectance and quantum efficiency measurements showed almost no difference between ITO thicknesses in the monofacial case, due to this highly angular distribution dependent behavior. On the other hand, for bifacial cells, a clear trend appears in favor of our reference thickness, where reflectance was improved at all angles. This was confirmed at cell level with reflectance and EQE measurements as well. In conclusion, this very different behavior of light management with respect of TCO thickness between monofacial and bifacial cases leads to different optimal thicknesses for each configuration. In our case, our reference thickness (~75 nm on textured substrate) gave the best results for bifacial cells.

Finally, the simulation and characterization results of the optical investigations led on bifacial cells were applied on SHJ devices. The gains observed in internal reflectance for a more transparent TCO layer translated well to  $J_{sc}$ , with a gain of 0.2 mA/cm<sup>2</sup> on our cells. Fill factor loss is 0.2%<sub>abs</sub> in average, without knowing with certainty whether this comes from the more resistive TCO or from the process variability. The cell efficiency increased by 0.1%, validating the interest of tuning the rear TCO properties to improve light trapping on bifacial cells (with a smaller grid pitch on the rear). Bifaciality also showed a small but repeatable gain, confirming the interest of this TCO optimization for all aspects of the cell performances.

For a further study, this work could be extended to TCO layers thinner than our reference, who could improve further the internal reflectance because of the smaller pathlength of light into the TCO, but could also be detrimental to lateral conductivity, even with a dense rear metal grid. Another promising aspect will be the integration of the optimized rear TCO layers on thinner SHJ cells, in order to assess if the improvement observed could be enhanced on thinner cells where more photons reach the rear side.

## REFERENCES

- [1] K. Yoshikawa et al., Nature Energy 2 (2017) 17032
- [2] A. Danel et al., Proceedings 31<sup>st</sup> European Photovoltaic Solar Energy Conference, (2013) 279-283.
- [3] M. Bivour et al., Solar Energy Materials and Solar Cells 122 (2014) 120-129.
- [4] Z. C. Holman et al., Journal of Applied Physics 113 (2013) 013107.
- [5] Yu et al., Japanese Journal of Applied Physics 57 (2018) 08RB15.
- [6] Y. S. Jung, Thin Solid Films 467 (2004) 36-42.
- [7] K. R. McIntosh, S. C. Baker-Finch, Proceedings 38<sup>th</sup> IEEE Photovoltaics Specialists Conference (2012).
- [8] H. A. Macleod, Thin-Film Optical Filters. Institute of Physics Publishing: London, 2001 (Chapter 2)
- [9] Z. C. Holman et al., Light: Science & Applications 2 (2013)